# Stability margin of the quadruped bionic robot with spinning gait[①]

Lei Jingtao(雷静桃)[②], Jiang Yunqi, Ren Mingming

(* School of Mechatronic Engineering and Automation, Shanghai University, Shanghai 200072, P. R. China)

## Abstract

Spinning gait is valuable for quadruped robot, which can be used to avoid obstacles quickly for robot walking in unstructured environment. A kind of bionic flexible body is presented for quadruped robot to perform the spinning gait. The spinning gait can be achieved by coordinated movement of body laterally bending and legs swing, which can improve the mobility of robot walking in the unstructured environments. The coordinated movement relationship between the body and the leg mechanism is presented. The stability of quadruped robot with spinning gait is analyzed based on the center of gravity (COG) projection method. The effect of different body bending angle on the stability of quadruped robot with spinning gait is mainly studied. For the quadruped robot walking with spinning gait, during one spinning gait cycle, the supporting polygon and the trajectory of COG projection point under different body bending angle are calculated. Finally, the stability margin of quadruped robot with spinning gait under different body bending angle is determined, which can be used to evaluate reasonableness of spinning gait parameters.

**Key words:** quadruped robot, bionic body, spinning gait, stability margin, body bending

## 0 Introduction

Bionic robotic is inspiring from the biological principles to imitate the structure, function and motion principles, and design the robots similar to the biological mobility.

As quadruped robots have several advantages, such as bood load performance, environment adaptability, less power consumption, having simpler structure as compared with six-legged or eight-legged robots, which have become a hot topic in the field of bionic robot.

For the quadruped robot, researchers have studied the straight walking gait, such as crawl gait, trot gait. Otherwise the terrain of the natural environment is complex, there are obstacles, moat, and so on. The quadruped robot should have spinning ability to avoid obstacles to improve the mobility of walking in unstructured environment.

For the spinning gait, one kind of style is just the leg swing. A rigid body is generally designed and does not the play the role in steering which leads to the turning radius relatively large, thus turning speed is slower. Zhang[1] presented a quadruped robot with multi-

ple locomotion modes. The omni-directional walking gait is analyzed. The simulation is performed to verify the validity of the omni-directional walking gait. As the rigid body is adopted, so its turning speed is slower. Wang[2] controled quadruped robot steering by adjusting the torque generated by the hip joint. The pitch angle of body is used to judge the stability. Roy[3,4] studied gait parameters of the hexapod robot turning in the unstructured environments. The turning of the six-legged robot is analyzed by coordination legs swing order, which leads to the turning radius relatively larger. The locomotion speed with turning gait is slower. An energy stability boundary method is adopted to analyze the stability of robot turning. Zhang[5] presented that the robot could achieve stable steering on a slope by increasing duty factor, thus the center of gravity of quadruped robot during the legs in the supporting phase could be dynamically moved.

It is difficult for the quadruped robot with rigid body to perform the spinning gait similar to the four-legged creatures. Recently, researchers have pay attention to the effect of the body in the turning gait. The rigid body is improved into a fore body and a rear body, and the rotating joint is designed to connect the two parts, which achieves relative rotating between the

two parts. This kind of body helps to improve the steering speed. Park[6,7] presented a kind of quadruped robot with waist joint called ELIRO, which connects the front body and rear body. The zigzag turning gait is analyzed, and the turning gait plan and stability based on the COG projection method was studied. Aoi[8] presented a kind of quadruped robot model whose front body and rear body were connected by a roll joint. By changing the stiffness of the roll joint, the robot could achieve gait transition. Kani[9] presented a kind of quadruped robot named Fanari with flexible body, which was inspired by the flexible trunk of the four-legged creatures. The effect of the spine flexibility on improving the stability is studied by the experimental method. A simulation model is also made in order to corroborate the experimental results of the robot. It is concluded that the robot with the spine that is flexible in both outward and downward directions, has the best stability, adaptability and fastest velocity in its gallop action. Lei[10,11] presented a kind of bionic body driven by PAMs, which could achieve the laterally bending and assist legs to perform the spinning gait of the quadruped robot inspired by the four-legged creatures, so as to improve the mobility of quadruped robot.

Compared with the traditional robot with rigid body, the robots are designed by increasing the body DOF to coordinate the leg mechanism and achieve the rotating gait. The quadruped robot with waist-joint can change the COG position by rotating the waist-joint. Thus the mobility and stability of robot can be easily guaranteed.

The quadruped robot should have the locomotion style of spinning gait to avoid the obstacles quickly. It is great significant to study the spinning gait of the quadruped robot, which will improve the mobility of the quadruped robot walking in the unstructured environment.

A quadruped robot with bionic flexible body is presented, which can bend and perform coordinated movement with legs so that the quadruped robot can achieve spinning gait. The kinematics of the body bending and the leg swing are derived, and then the coordinated motion relationship between the body and legs are analyzed. For the quadruped robot performs one spinning gait, the supporting area and the trajectory of the COG projection point changing with different bending angles of the flexible body are calculated. Finally, the stability margin of the robot during the spinning gait based on the COG projection method is analyzed, which can be used to determine the reasonable spinning gait parameters.

# 1  Biological body and bionic body

## 1.1  Biological body

The highly flexible biological body of four-legged creatures plays an important role for its spinning gait, high-speed running or jumping locomotion and the dynamic stability.

The body movement of the four-legged creature is that of the spine driven by the contraction of paraspinal muscles. The spine is composed of several rigid spine vertebrae connected by passive ligaments, and there are several intervertebral disc. The spine structure makes the biological body have flexible bending properties with the terrain and locomotion speed.

## 1.2  Quadruped robot

The super athletic ability of the four-legged creatures will provide a good biology template for developing the quadruped bionic robot, which is the result of the work together with the nervous system, muscular system and skeletal system. Generally, the trunk of the four-legged creature is flexibility, which is obviously observable while running.

The quadruped robot is composed of four legs and one bionic flexible body driven by the pneumatic artificial muscles (PAMs). The structure of four legs is the same. Each leg is designed with three rotating joints, which are side-swing hip joint, forward-swing hip joint and knee joint, as shown in Fig. 1.
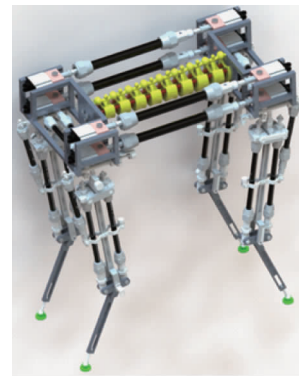


**Fig. 1**　Quadruped robot

## 1.3  Bionic flexible body

The biological body is a complex system. The vertebrae are separated by the intervertebral discs. Several rigid vertebrae are connected by the muscles and ligaments. Thus the structure makes the trunk have the characteristic of flexibility. The coordinated movement of the trunk and the legs can achieve the spinning gait of the creature. The biological structure of trunk will provide reference model for developing the

rigid-flexible coupling body of the quadruped bionic robot.

Based on the dynamic bending principles of the biological body for the four-legged creature adapting to the unstructured environment, the rigid-flexible coupling bionic body for quadruped robot is presented to improve the traditional rigid body, which follows the design principles of light weight and bionic. The body is driven by PAMs, which could bend with different stiffness to meet the need of spinning gait and high-speed locomotion of quadruped robot.

Musculoskeletal bionic body mechanism of quadruped robot is composed of front body, rear body, bionic spine and four PAMs. The end of the PAM is designed with a miniature cylinder to compensate for the PAM contraction in the other side. The front body and rear body are connected by the PAMs and the bionic spine, where PAMs drive the bionic spine bending to produce the relatively rotating movement between the front body and the rear body.

The bionic spine of the body is designed with 10 bionic spinal units, which is composed of biomimetic vertebra, intervertebral disc and three springs. The bionic spinal units connect each other and form 9 passive joints. The intervertebral disc is located in the middle of two biomimetic vertebrae. Three springs pass through the intervertebral disc and connect two adjacent biomimetic vertebrae[10].

### 1.4 Bionic body bending for the spinning gait

The bionic body has the variable stiffness characteristic by changing the inner gas pressure of the PAMs, which could easily bend the body with different angle. The coordinated movement between the body bending and the legs swing could achieve spinning gait of quadruped robot.

## 2 Spinning gait

Some assumptions for analyzing the spinning gait of quadruped robots are as follows:

(1) During the process of the spinning, the height of the body and the ground keep unchanged.

(2) During the process of the spinning, when the body bends, the length of the bionic spine centerline keeps unchanged.

(3) During the process of the spinning, the slip between the foot and the ground need not to be considered.

The spinning gait is a kind of the walking gait for the quadruped robot. The diagram of the spinning gait of quadruped robot is shown in Fig. 2, and the sequence of the robot leg swing finishing one time spinning counter-clockwise is 2-1-3-4.

Repeating the movement shown in Fig. 2, the robot can achieve spinning gait with one cycle. Thus the robot can achieve rotating around its center and an omni-directional walking. The proposed spinning gait has the following features:

(1) The body bending and the leg swing should be controlled simultaneously, thus, the spinning speed could be improved.

(2) As there are three legs in the supporting phase at the same time, it belongs to static gait. If the gait parameters are reasonable, then the robot could keep the stability in spinning gait.

(3) The center of the robot turning direction of the robot is located in the center of the bionic body. The robot turns direction around its center.
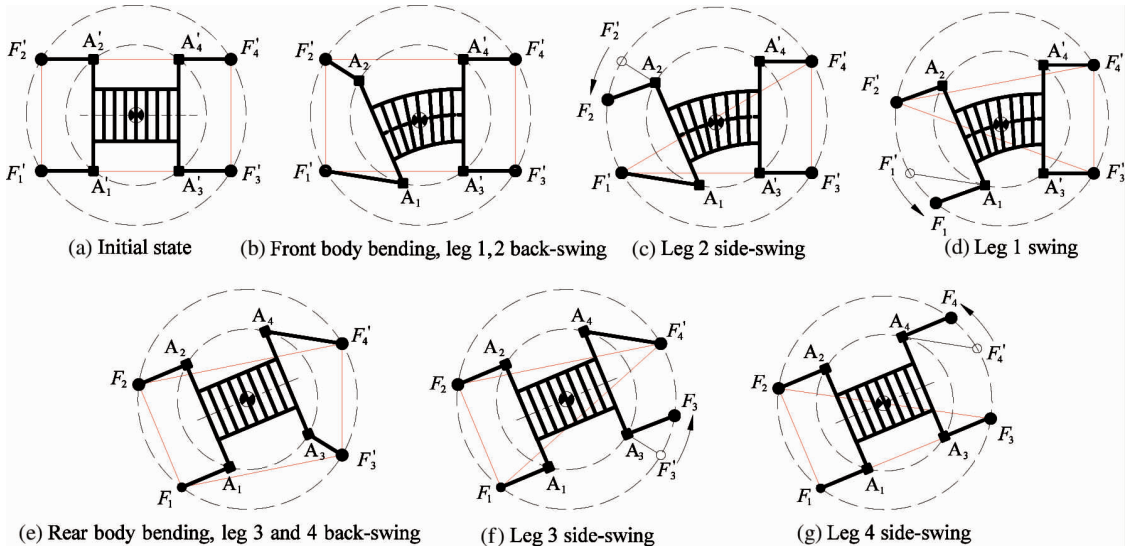


(a) Initial state    (b) Front body bending, leg 1,2 back-swing    (c) Leg 2 side-swing    (d) Leg 1 swing

(e) Rear body bending, leg 3 and 4 back-swing    (f) Leg 3 side-swing    (g) Leg 4 side-swing

**Fig. 2**    Diagram of the spinning gait

# 3    Coordinated movement of body and legs

## 3.1    Body bending and legs swing

When the quadruped robot walks with spinning gait, the body bending and legs in side-swing or back-swing should keep the coordinated movement so that the robot could keep stability with the spinning gait.

After the body bending, the leg follows it and begins to side-swing. While the leg finishes the side-swing, it should keep the vertical state to the body, as shown in Fig. 3.
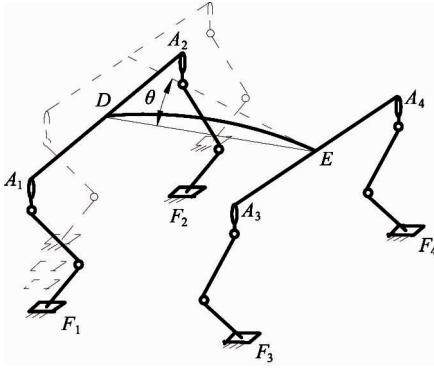
**Fig. 3**    Body bending and legs swing

Firstly, the range of the body bending and the leg swing should be determined. The maximum bending angle of the body is restricted by the following factors.

The minimum shrink length of the PAM. The body bending angle is related to the PAM initial length and its shrinkage rate.

The movement range of the hip joint with the supporting leg back-swing.

The movement range of the leg side-swing. After the body bending, the leg begins side-swing until the leg keeps vertical with the body. The maximum movement range of the leg side-swing or back-swing is determined by the structural parameters of the leg.

Thus the maximum bending angle of the body can be determined.

## 3.2    Kinematics of the leg side-swing

The D-H coordinate systems of the leg side-swing are shown in Fig. 4. Two coordinate systems $\{A_{Li}\}$ ($x_{ALi}$  $y_{ALi}$  $z_{ALi}$) and $\{1\}$ ($x_1$  $y_1$  $z_1$) are located at Joint 1. The coordinate system $\{2\}$ ($x_2$  $y_2$  $z_2$) and $\{3\}$ ($x_3$  $y_3$  $z_3$) are located at Joint 2 and the Joint 3, respectively. $\theta_1$, $\theta_2$, $\theta_3$ are joint variables. $l_1$, $l_2$, $l_3$ are the length of link 1 of leg, thigh leg and the shank leg, respectively.
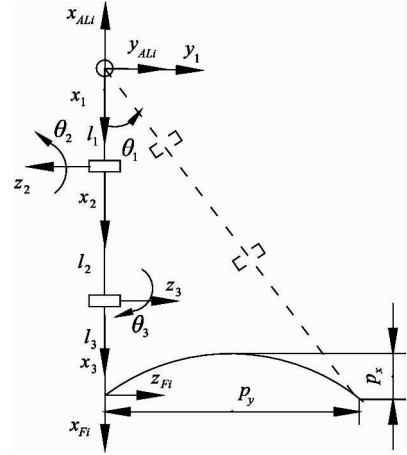
**Fig. 4**    D-H coordinate system of the leg side-swing

$$
{}^{A_{Li}}_{F_i}\mathbf{T} = {}^{A_{Li}}_{1}\mathbf{T}(\theta_1) \cdot {}^{1}_{2}\mathbf{T}(\theta_2) \cdot {}^{2}_{3}\mathbf{T}(\theta_3) \cdot {}^{3}_{F_i}\mathbf{T}
$$

$$
= \begin{bmatrix} c_1 s_2 s_3 + c_1 c_2 c_3 & c_1 s_2 c_3 - c_1 c_2 s_3 & -s_1 & p_{ix} \\ s_1 s_2 s_3 + s_1 c_2 c_3 & s_1 s_2 c_3 - s_1 c_2 s_3 & c_1 & p_{iy} \\ s_2 c_3 - c_2 s_3 & -c_2 c_3 - s_2 s_3 & 0 & p_{iz} \\ 0 & 0 & 0 & 1 \end{bmatrix}
$$

$$\tag{1}$$

where, $s_i = \sin\theta_i$, $c_i = \cos\theta_i$.

$$
\begin{cases} p_{ix} = l_1 c_1 + l_3 c_1 (s_2 s_3 + c_2 c_3) + l_2 c_1 c_2 \\ p_{iy} = l_3 s_1 (s_2 s_3 + c_2 c_3) + l_1 s_1 + l_2 s_1 c_2 \\ p_{iz} = l_2 s_2 - l_3 (c_2 s_3 - s_2 c_3) \end{cases}
$$

As the coordinate systems of side-swing hip joint on the body and on the leg are different, so the position and orientation between two coordinates systems can be expressed as

$$
{}^{A_i}_{A_{Li}}\mathbf{T} = \begin{bmatrix} 0 & 0 & -1 & 0 \\ 0 & 1 & 0 & 0 \\ 1 & 0 & 0 & 0 \\ 0 & 0 & 0 & 1 \end{bmatrix}
$$

Then the position and orientation of the foot with respect to the body is

$$
{}^{B_0}_{F_i}\mathbf{T} = {}^{B_0}_{A_i}\mathbf{T} \cdot {}^{A_i}_{H_i}\mathbf{T} \cdot {}^{H_i}_{1}\mathbf{T} \cdot {}^{1}_{2}\mathbf{T} \cdot {}^{2}_{3}\mathbf{T} \cdot {}^{3}_{F_i}\mathbf{T}
$$

## 3.3    Rotating range of the hip joint

On one hand, the side-swing hip joint moves with the body bending. Meanwhile, the side-swing hip joint moves with the back-swing of the leg in the supporting phase. So the movement of the hip joint is restricted by the maximum bending range of body and maximum back-swing range of leg in supporting phase. Therefore, the intersection of the movement range of the hip joint in the body and the leg is the maximum movement range of the hip joint.

Take leg 1 as example, the hip joint movement is derived as follows.

3.3.1    Hip joint movement range with leg back-swing

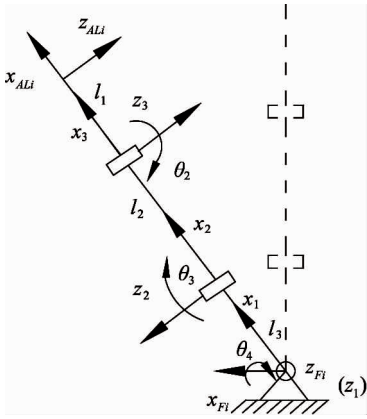The leg is in the supporting phase and begins to back-swing with the body bending, as shown in Fig. 5.



**Fig. 5** D-H coordinate systems of leg back-swing

$$\begin{aligned}
{}^{F_i}_{A_i}\mathbf{T} &= {}^{F_i}_{A_{Li}}\mathbf{T} \cdot {}^{A_i}_{A_{Li}}\mathbf{T}^{-1} \\
&= \begin{bmatrix}
-s_4 & c_4\cos(\theta_2-\theta_3) & c_4\sin(\theta_3-\theta_2) & p_{Aix} \\
c_4 & s_4\cos(\theta_2-\theta_3) & s_4\sin(\theta_3-\theta_2) & p_{Aiy} \\
0 & \sin(\theta_3-\theta_2) & -\cos(\theta_2-\theta_3) & p_{Aiz} \\
0 & 0 & 0 & 1
\end{bmatrix}
\end{aligned}$$

$$(2)$$

where,

$$\begin{cases}
p_{Aix} = (l_1\cos(\theta_3-\theta_2)+l_2c_3+l_3)c_4 \\
p_{Aiy} = (l_1\cos(\theta_2-\theta_3)+l_2c_3+l_3)s_4 \\
p_{Aiz} = l_1\sin(\theta_3-\theta_2)+l_2s_3
\end{cases}$$

Coordinate system $\{A'_1\}$ is the initial coordinate system of the hip joint. The hip joint moves from point $A'_1$ to $A_1$.

According to the coordinate transformation Eq. (2), the position vector of hip joint $A_1$ in the leg mechanism in the horizontal plane is

$$\begin{cases}
p_{A_{1x}} = -(l_1\cos(\theta_3-\theta_2)+l_2c_3+l_3)c_4 \\
p_{A_{1y}} = l_2s\theta_3 - l_1s(\theta_2-\theta_3)
\end{cases}$$

$$(3)$$

As the bionic leg driven by PAMs, the joint rotating range is restricted by the PAMs length and its shrinkage rate. The rotating range of each joint is as follows:

$$\theta_1 \in [0°, 30°], \quad \theta_2 \in [10°, 20°],$$
$$\theta_3 \in [-5°, 75°], \quad \theta_4 \in [90°, 120°].$$

According to the rotating range of the joints, the movement range of the hip joint with leg back-swing can be calculated by Eq. (3):

$$p_{A1x} \in [0, 300]\,\text{mm}, \quad p_{A1y} \in [-150, 0]\,\text{mm}.$$

### 3.3.2 Hip joint in the body

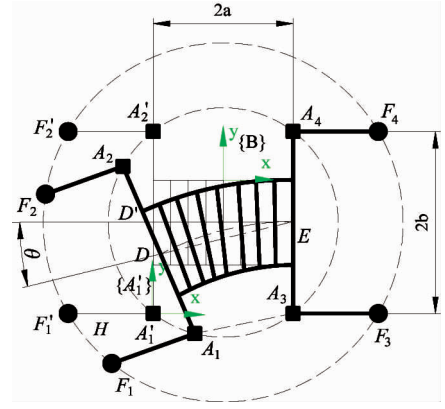The body bending and the leg swing are shown in Fig. 6.



**Fig. 6** Hip joint moves with the body bending

The hip joint moves from point $A'_1(x_{A1'},\ y_{A1'})$ to point $A_1(x_{A1},\ y_{A1})$ with the body bending.

The displacements of the hip joint along $x$-axis and $y$-axis are

$$\begin{cases}
p_{A1x} = 2a + b\sin2\theta - \dfrac{a\sin2\theta}{\theta} \\
p_{A1y} = b - b\cos2\theta - \dfrac{a}{\theta} + \dfrac{a\cos2\theta}{\theta}
\end{cases}$$

$$(4)$$

According to Eqs (3) and (4), the movement of the hip joint in the horizontal plane $XOY$ is calculated as shown in Fig. 7. The line indicates the trajectory of the hip joint with the body bending angle at 10°. The other line indicates the trajectory of the hip joint with the body bending angle at 20°. The dark area indicates the movement range of the hip joint with leg back-swing.
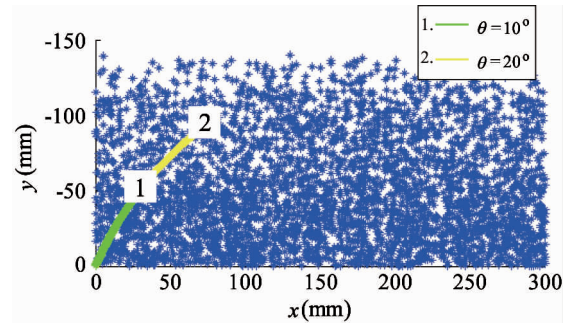


**Fig. 7** Movement range of the hip joint

Considering the initial length and the shrinkage rate of PAM, the move range of the leg side-swing and back-swing, the body bend angle range, the maximum bending angle of the body could reach 20°.

## 4 Stability analysis

About the study on the stability of walking robots, many stability criteria have been defined, which is divided into static stability and dynamic stability. The

static stability methods include COG projection method[12], longitudinal stability margin[13], energy stability margin (ESM) method[14], normalized energy stability margin (NESM) method[15], and so on. The dynamic stability methods include zero moment point (ZMP) method[16], center of pressure method[17], dynamic stability margin (DSM)[18], and so on.

As the spinning gait planned in this work, the spinning speed is slower, and the inertial force has less influence on the stability. For the quadruped robot walks with the spinning gait, there are three legs in the support phase, so it belongs to the static stability.

## 4.1 Stability margin

The COG projection method is used to analyze the stability of quadruped robot with spinning gait. When the quadruped robot walks with spinning gait, the feet in the supporting phase in the horizontal plane form a supporting polygon. When the COG projection point $G$ of the quadruped robot locates inside the supporting polygon, the robot is static stable, otherwise the robot is unstable.

Definition: the vertical distance from the COG projection point $G$ to each side of the supporting polygon, where the minimum distance is defined as the stability margin, expressed by $S_m$. $S = \min(d_i, d_j, d_k)$, as shown in Fig. 8.
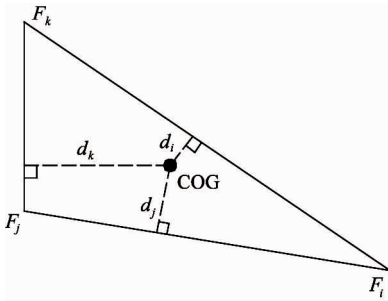


**Fig. 8** Stability margin

Setting the coordinates of the supporting feet as $F_i(x_{Fi}, y_{Fi}, z_{Fi})$, $F_j(x_{Fj}, y_{Fj}, z_{Fz})$, $F_k(x_{Fk}, y_{Fk}, z_{Fk})$, and the COG projection point is $G(x_G, y_G, z_G)$.

During the quadruped robot walk in with the spinning gait, the coordinate of the supporting feet can be calculated by Eq. (1).

Assuming the shortest distance is from the COG projection point to the side of $F_k F_i$, then the stability margin is

$$S_m = \frac{|(x_{Fk} - x_{Fi})(y_G - y_{Fk}) - (y_{Fk} - y_{Fi})(x_G - x_{Fk})|}{\sqrt{(x_{Fk} - x_{Fi})^2 + (y_{Fk} - x_{Fi})^2}}$$

(5)

## 4.2 Coordinates of COG projection point

The quadruped robot is composed of the fore body, rear body, bionic spine and four legs. The coordinate of the front body centroid $D(x_D, y_D)$ is

$$\begin{cases} x_D = a - \dfrac{a \sin 2\theta}{\theta} \\ y_D = \dfrac{a(\cos 2\theta - 1)}{\theta} \end{cases}$$

The vertebra number is $w$, whose centroid coordinate $J(x_J, y_J)$ is

$$\begin{cases} x_J = x_D + (\dfrac{l_1}{2\theta} \sin\theta_0 - \dfrac{l_1}{2\theta} \sin\theta_w) \\ y_J = y_D + (\dfrac{l_1}{2\theta} \cos\theta_w - \dfrac{l_1}{2\theta} \cos\theta_0) \end{cases}$$

After the rear body bending, the coordinate of the rear body centroid $E(x_E, y_E)$ is

$$\begin{cases} x_E = \dfrac{a(\theta - \sin\theta)}{\theta} + \dfrac{2a \cos\theta(\cos(\theta - 2\beta) - 1)}{2\theta - 2\beta} \\ y_E = \dfrac{a(\cos\theta - 1) + 2a\theta(\sin(3\theta - 2\beta) - 1)}{(2\theta - 2\beta)\theta} \end{cases}$$

Then the coordinate of COG projection point $G$ is

$$\begin{cases} x_G = \dfrac{\sum\limits_{n=1}^{4} \sum\limits_{q=1}^{3} m_{nq} x_{nq} + m_D x_D + m_E x_E + m_J x_J}{\sum\limits_{n=1}^{4} \sum\limits_{q=1}^{3} m_{nq} + m_J} \\ \\ y_G = \dfrac{\sum\limits_{n=1}^{4} \sum\limits_{q=1}^{3} m_{nq} y_{nq} + m_D y_D + m_E y_E + m_J y_J}{\sum\limits_{n=1}^{4} \sum\limits_{q=1}^{3} m_{nq} + m_J} \end{cases}$$

(6)

where, $n$ is the $n$th leg of the quadruped robot, $q$ is the link of the leg, $m_{nq}$ is the link mass. $(x_{nq}, y_{nq})$ is the center coordinates of each link. $m_D$ is the mass of front body, and $m_E$ is the mass of bear body, $m_J$ is the mass of vertebra.

## 4.3 Supporting area and stability margin

When the quadruped robot walks with spinning gait, the body bending angle is closely related to its stability. The supporting area, the trajectory of the COG projection point and the stability margin changing with the body bending angle will be calculated, and the stability will be analyzed comparatively under different body bending angle.

The structure and gait parameters of the quadruped robot are shown in Table 1.

Table 1    Parameters of quadruped robot

| Parameter | Symbol | Value | Unit |
|---|---|---|---|
| Length of link 1 | $l_1$ | 50 | mm |
| Length of link 2 | $l_2$ | 200 | mm |
| Length of link 3 | $l_3$ | 150 | mm |
| Body length | $a$ | 190 | mm |
| Body width | $b$ | 90 | mm |
| Body height | $c$ | 50 | mm |
| Mass of link 1 | $m_1$ | 0.628 | kg |
| Mass of link 2 | $m_2$ | 2.512 | kg |
| Mass of link 3 | $m_3$ | 1.884 | kg |
| Body mass | $m_c$ | 5.024 | kg |
| Vertebra number | $w$ | 10 | |
| Vertebra mass | $mi$ | 0.01 | kg |
| Gait cycle | $T$ | 30 | s |
| PAM initial length | $L_0$ | 200 | mm |
| PAM installing size | $d$ | 40 | mm |

According to the structural parameters of the quadruped robot, the step distance is 0mm ~ 140mm, and the step height is 0mm ~ 100mm. For calculating the trajectory of the COG projection point and the stability margin, the same step height 30mm is adopted for different body bending angle. The step distance changes with the different body bending angle. When the body bending angle is 5°, 10°, 15°, 20°, the step distance is 40mm, 60mm, 80mm and 100mm, respectively.

For the quadruped robot performs one continuous spinning gait, the supporting area and the trajectory of the COG projection point under different body bending angle of 5°, 10°, 15°, 20° are shown in Fig.9(a) ~ (d). Different colors are used to express the changing process of the supporting area, the changing order is ①②③⑤⑤⑥.
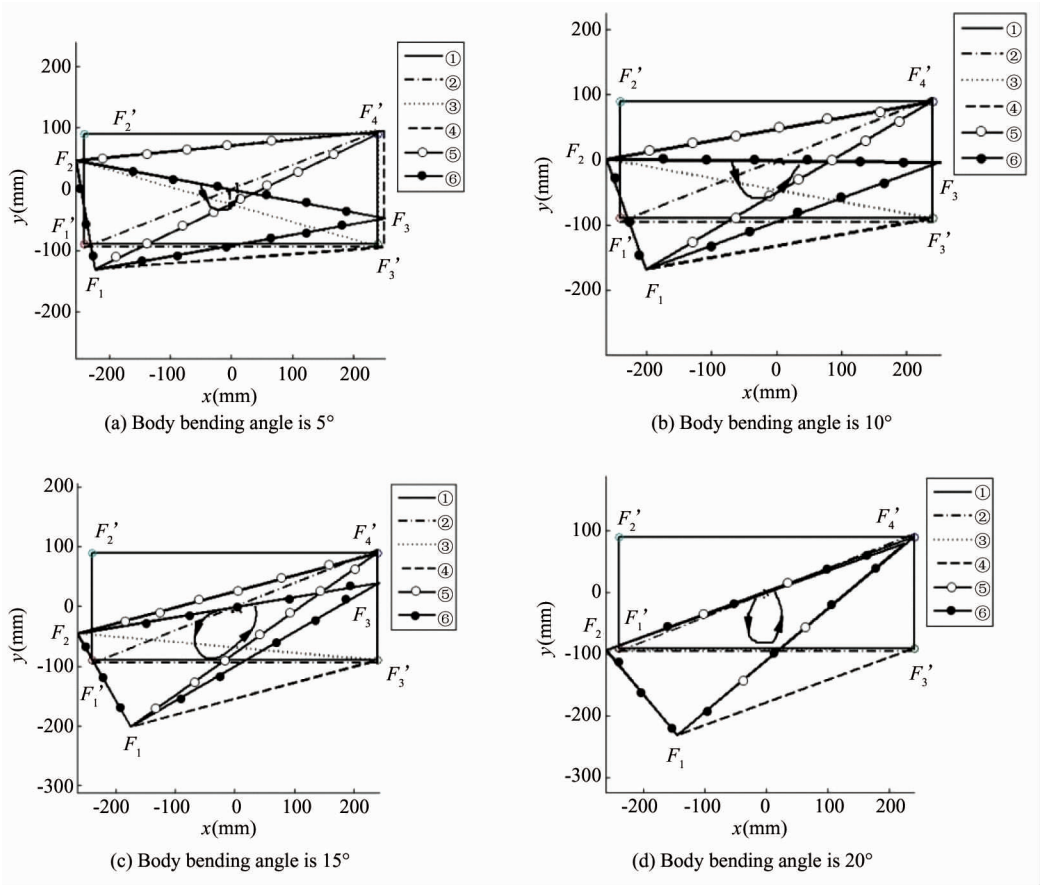


(a) Body bending angle is 5°

(b) Body bending angle is 10°

(c) Body bending angle is 15°

(d) Body bending angle is 20°

Fig.9    Supporting area and the trajectory of COG projection point during the quadruped robot spinning

For the quadruped robot performs one continuous spinning gait, assuming the body bending angle is 25°, the supporting area and the trajectory of the COG projection point are shown in Fig.10. It can be seen that COG projection point G falls outside the supporting area, which indicates that the robot is unstable.

For the quadruped robot walking with the spinning robot under different body bending angles of 5°, 10°, 15°, 20° and 25°, the stability margin changing with time is calculated, as shown in Fig.11.
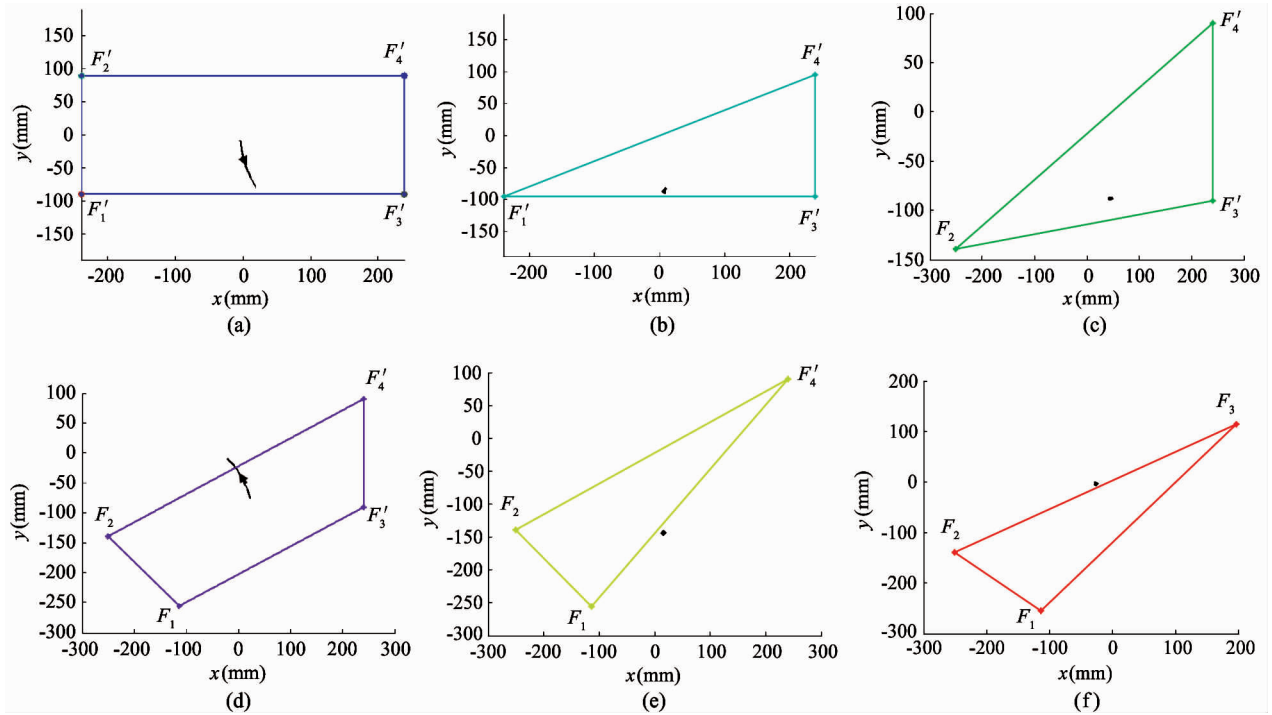
**Fig. 10** Supporting area and the trajectory of COG projection point changing during spinning of the quadruped robot
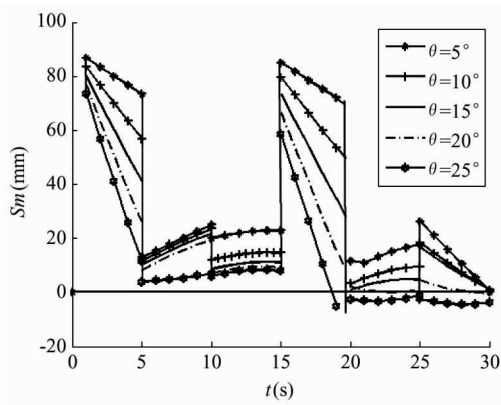


**Fig. 11** Stability margin changes with time under different body bending angle

It can be concluded that the stability margin decreases with the body bending angle increasing. When the body bend angles greater than 20°, the stability margin is less than zero, which show that the robot is unstable.

According to the structural parameters of the quadruped robot, when the body bending angle is less than 20°, which is in the motion range of the leg mechanism, thus the body and the legs could keep coordinated movement, and the robot could keep stable spinning gait. Otherwise, when the body bending angle greater than 20°, the robot couldn't keep stable spinning.

The bending characteristic of the flexible body can improve the steering flexibility and rapidness, which is

helpful for the quadruped robot to avoid the obstacle quickly.

## 5   Conclusions

The spinning gait of quadruped robot and its stability is studied to improve the locomotion mobility walking in the unstructured environments.

The body bending angle is determined to achieve stable spinning gait according to the structure parameters and the coordinated movement between the body and legs. The coordinate movement of the flexible body and the legs for the spinning gait of quadruped robot is analyzed. The kinematics of the flexible body bending and the leg swing are analyzed, and then the movement range of the hip joint in the body bending and the leg swing can be determined. The maximum bending angle of the body is determined. The stability of the quadruped robot with the spinning gait is analyzed by the COG projection method. For the quadruped robot performs one time of continuous spinning gait, the supporting area and the trajectory of the COG projection point are comparatively analyzed under different body bending angle. Finally, the stability margin change with time during one spinning gait under different body bending angle is obtained, which can be used to determine reasonable spinning gait parameters and suitable body bending angle.

Future work will focus on the variable stiffness

characteristic of the bionic body, the influence of the body stiffness on the stability of the quadruped robot, and the experiments on the stability of the spinning gait.

## References

[ 1 ] Zhang F H, Wu W G, Lang Y D, et al. Omni-directional quadruped walking gaits and simulation for a gorilla robot. In: Proceedings of the IEEE/RSJ International Conference on Intelligent Robots and Systems, Edmonton, Canada, 2005. 1121-1126

[ 2 ] Wang X, Li M, Wang P, et al. Running and turning control of a quadruped robot with compliant legs in bounding gait. In: Proceedings of the IEEE International Conference on Robotics and Automation, Shanghai, China, 2011. 511-518

[ 3 ] Roy S S, Pratihar D K. Soft computing-based expert systems to predict energy consumption and stability margin in turning gaits of six-legged robots. *Expert Systems with Applications*, 2012, 39(5):5460-5469

[ 4 ] Roy S S, Pratihar D K. Effects of turning gait parameters on energy consumption and stability of a six-legged walking robot. *Robotics and Autonomous Systems*, 2012, 60 (1):72-82

[ 5 ] Zhang L, Wang L, Ma S, et al. Research of a quadruped robot walking on a slope based on 4-leg supporting period. In: Proceedings of the IEEE International Conference on Robotics and Biomimetics, Tianjin, China, 2010. 1346-1351

[ 6 ] Park S H, Kim D S, Lee Y J. Discontinuous spinning gait of a quadruped walking robot with waist-joint. In: Proceedings of the IEEE/RSJ International Conference on Intelligent Robots and Systems, Beijing, China, 2005. 2744 – 2749

[ 7 ] Park S H, Lee Y J. Discontinuous zigzag gait planning of a quadruped walking robot with a waist-joint. *Advanced robotics*, 2007, 21(1-2):143-164

[ 8 ] Aoi S, Yamashita T, Ichikawa A, et al. Hysteresis in gait transition induced by changing waist joint stiffness of a quadruped robot driven by nonlinear oscillators with phase resetting. In: Proceedings of the IEEE/RSJ International Conference onIntelligent Robots and Systems, Taipei, China, 2010: 1915-1920

[ 9 ] Kani M H H, Derafshian M, Bidgoly H J, et al. Effect of flexible spine on stability of a passive quadruped robot: Experimental results. In: Proceedings of the IEEE International Conference on Robotics and Biomimetics, Phuket, Thailand, 2011. 2793-2798

[10] Lei J T, Yu H Y, Wu Z Z. Analysis on pivot turning of quadruped robot with bionic flexible body driven by the PAMs. *High Technology Letters*, 2014, 20(3):288-294

[11] Lei J T, Yu H Y, Wang T M. Dynamic bending of bionic flexible body driven by PAMs for spinning gait of quadruped robot. *Chinese Journal of Mechanical Engineering*, 2016, 29(1):11-20

[12] Yi S. Stable Walking of Quadruped Robot by Impedance Control for Body Motion. *International Journal of Control & Automation*, 2013, 6(2):99-110

[13] De Santos P G, Estremera J, Garcia E, et al. Including joint torques and power consumption in the stability margin of walking robots. *Autonomous Robots*, 2005, 18(1): 43-57

[14] Garcia E, De Santos P G. An improved energy stability margin for walking machines subject to dynamic effects. *Robotica*, 2005, 23(1):13-20

[15] Hirose S, Tsukagoshi H, Yoneda K. Normalized energy stability margin and its contour of walking vehicles on rough terrain. In: Proceedings of the IEEE International Conference on Robotics and Automation, Seoul, Korea, 2001. 181-186

[16] Zhang S, Gao J, Duan X, et al. Trot pattern generation for quadruped robot based on the ZMP stability margin. In: Proceedings of the IEEE International Conference on Complex Medical Engineering, Beijing, China, 2013. 608-613

[17] Wang P F, Sun L N. The stability analysis for quadruped bionic robot. In: Proceedings of the IEEE/RSJ International Conference on Intelligent Robots and Systems, Beijing, China, 2006. 5238-5242

[18] Besseron G, Grand C, Amar F B, et al. Decoupled control of the high mobility robot hylos based on a dynamic stability margin. In: Proceedings of the IEEE/RSJ International Conference on Intelligent Robots and Systems, Nice, France, 2008. 2435-2440

**Lei Jingtao**, born in 1970. She received her Ph. D degrees from Beihang University in 2007. She also received her B. S. and M. S. degrees from Henan University of Science and Technology in 1991 and 1996 respectively. Her research interests include the bionic robot.